NEW EVIDENCE FOR AN N = 32 SUBSHELL

J.I. Prisciandaro, P.F. Mantica, B.A. Brown, D.W. Anthony, M.W. Cooper[a], A. Garcia[b], D.E. Groh, A. Komives[b], W. Kumarasiri, P.A. Lofy, A.M. Oros-Peusquens, S.L. Tabor[a] and M. Wiedeking[a]

Based on self-consistent energy density calculations, Tondeur [1] proposed $N = 32$ as a new magic number for neutron-rich nuclides. Following the beta decay of ^{52}K, Huck *et al.* [2] assigned the 2.56 MeV state in $^{52}_{20}$Ca$_{32}$ a spin and parity of 2^+. As compared to the first excited 2^+ level in ^{50}Ca, an increase in $E(2^+_1)$ was observed. Huck *et al.* [2] suggested the rise at $N = 32$ was due to the $\nu 2p_{3/2}$ subshell closure, indicating that $N = 32$ was semi-magic. This assertion was consistent with Tondeur's theoretical prediction [1]. To determine whether $E(2^+_1)$ peaks at $N = 32$ for calcium, the $E(2^+_1)$ systematics of heavier calcium isotopes would be of value. However, at present these nuclei are difficult to produce with sufficient statistics. Therefore, the systematics of the chromium isotopes were examined. Similar to $^{52}_{20}$Ca$_{32}$, the first 2^+ state of $^{56}_{24}$Cr$_{32}$ lies higher in energy relative to its $N-2$ neighbor, ^{54}Cr$_{30}$. Unlike ^{52}Ca$_{32}$, the spin and parity assignment of the 2^+ level for ^{56}Cr$_{32}$ was deduced from the shape of proton angular distribution curves following its production via the (t,p) reaction [3]. A second (t,p) study confirmed the spin-parity assignments for a number of states, including the first excited 2^+ state at 1007 keV [4]. To determine whether the first excited 2^+ energies continued to rise or peaked at $N = 32$, it was necessary to measure $E(2^+_1)$ values beyond $N = 32$. In this report, the energy of the first excited 2^+ state of ^{58}Cr is presented.

To study the low-energy properties of ^{58}Cr, the parent nuclide, ^{58}V, along with several other neutron-rich nuclides were produced via projectile fragmentation of a 70 MeV/nucleon ^{70}Zn beam in a ^{9}Be target at the National Superconducting Cyclotron Laboratory at Michigan State University. The fragments of interest were separated from other reaction products using the A1200 fragment analyzer. Further separation was achieved by passing the radioactive beam through the Reaction Products Mass Separator (RPMS). The new beta detection system discussed in Ref. [5] was used for this study. Implant events were identified and correlated with subsequent β decays in the double-sided Si strip detector (DSSD). Each implant and decay event was tagged with an absolute time stamp. The half-lives of decaying species were deduced by taking the difference between the absolute time of a fragment implant and its subsequent beta decay. In addition, beta-delayed gamma rays were monitored by an array of three Ge clover detectors and two high purity Ge detectors that surrounded the implantation detector.

To deduce the decay properties of ^{58}V, a gate was defined in the energy loss versus time of flight spectrum. A $T^{\beta}_{1/2}$ = 180(36) ms was extracted by fitting the data in Fig. 1a with a one component exponential with background. A lifetime curve was also obtained by correlating ^{58}V fragments with beta-delayed gamma rays of energy 880 keV (see discussion below). Considering this half-life, $T^{\beta-\gamma}_{1/2}$ = 218(30) ms, along with $T^{\beta}_{1/2}$, an adopted half-life of 202(36) ms was obtained for the decay of ^{58}V. This half-life is consistent with previous measurements performed by Sorlin *et al.* [6], $T_{1/2}$ = 205(20) ms, and Ameil *et al.* [7], $T_{1/2}$ = 200(20) ms. In addition, a single peak was observed at 879.9(2) keV in the beta-delayed gamma ray spectrum below 1.5 MeV (see Fig. 1b). This result is in general agreement with the work of Sorlin *et al.* [6] who observed a broad peak at 900(100) keV in BGO scintillator detectors following the beta-delayed gamma emission of ^{58}V. This 900-keV transition had a FWHM approximately twice that of other transitions observed in their BGO detectors. The authors proposed this peak as a doublet, which may contain the $4^+ \rightarrow 2^+ \rightarrow 0^+$ cascade. However, no evidence for a second transition in the range 800 - 1000 keV, with similar intensity to the 880-keV gamma ray, was observed in the present study.

The first excited 2^+ energies of neutron-rich chromium isotopes in the range $N = 28 - 36$ are shown in Fig. 2, where the data were obtained from Ref. [8, 9, 10, 11]. As compared to ^{54}Cr$_{30}$ and the new measurement for ^{58}Cr$_{34}$, there is a clear rise in $E(2^+_1)$ for ^{56}Cr$_{32}$. This peak in the $E(2^+_1)$ value for ^{56}Cr$_{32}$ provides empirical

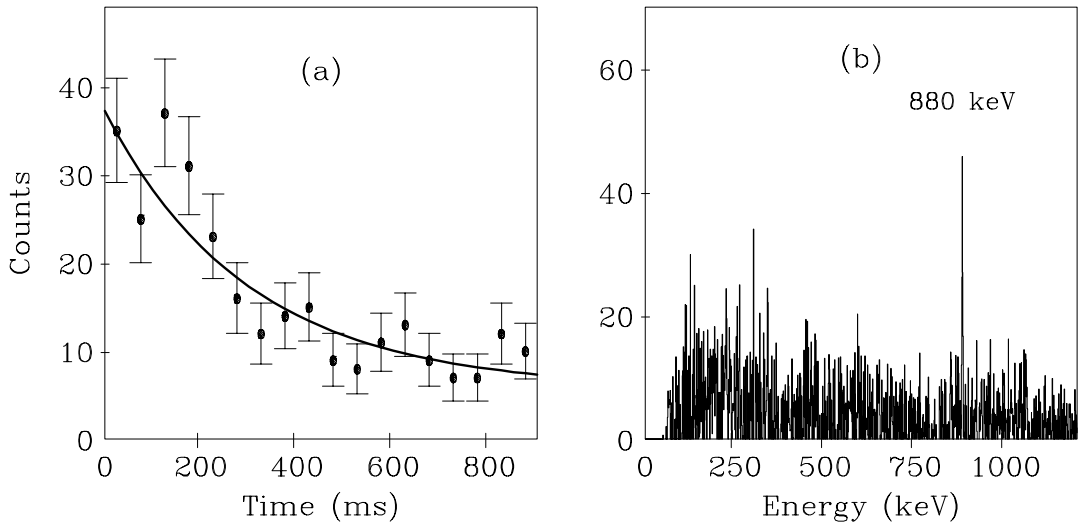

Figure 1: (a) Extracted ^{58}V life-time curve following the correlation of ^{58}V implants and subsequent β-decays. (b) Beta delayed gamma ray spectrum following the decay of ^{58}V.

evidence for a significant subshell gap at $N = 32$.

Tu *et al.* [12] attributed the increase in binding at $N = 32$ for ^{52}Ca to the $Z = 20$ shell closure. However, based on the present measurement, a peak in $E(2_1^+)$ is now seen for ^{56}Cr$_{32}$, which resides in the middle of the $Z = 20 - 28$ shell. In addition, although $E(2_1^+)$ values increased at $N = 32$ for the calcium isotopes, this behavior is not observed for nickel (see Fig. 2), which has a proton closed shell. If the strength of $N = 32$ were reinforced by a proton shell closure, a similar peak in $E(2_1^+)$ would be expected for ^{60}Ni. An alternative explanation for the appearance of the $N = 32$ subshell for neutron-rich systems is to consider a change in the proton-neutron monopole interaction strength. According to Federman and Pittel [13], the proton-neutron interaction is strongest when the orbitals they occupy strongly overlap. The overlap between the proton and neutron orbitals is maximum when $\ell_n \approx \ell_p$ [13]. Therefore, when $Z = 28$, the $1f_{7/2}$ orbital is filled and the $\pi 1f_{7/2}$ - $\nu 1f_{5/2}$ interaction should be strong, depressing the energy of the $\nu 1f_{5/2}$ orbital [14]. As protons are removed from the $1f_{7/2}$ orbital, the $\pi 1f_{7/2}$ - $\nu 1f_{5/2}$ interaction weakens. When $Z = 20$, no protons occupy the $1f_{7/2}$ orbital in the ground state, thus the $\pi 1f_{7/2}$ - $\nu 1f_{5/2}$ interaction should be diminished. This reduced monopole interaction, and the significant $2p_{1/2} - 2p_{3/2}$ spin-orbit energy splitting, results in the emergence of the $N = 32$ subshell.

Shell-model calculations in the region $N = 28 - 40$ and $Z = 20 - 28$ were carried out in a *pf*-shell model space with an FPD6 effective interaction [15]. For the Ca isotopes the full basis calculation is feasible. The calculated energies of the lowest 2^+ states in the Ca isotopes are (in MeV) 3.66 (^{48}Ca), 1.33 (^{50}Ca), 2.75 (^{52}Ca), 1.47 (^{54}Ca), 1.37 (^{56}Ca) and 1.30 (^{58}Ca). The agreement with the experimental values in ^{48}Ca, ^{50}Ca and ^{52}Ca is good. The high energy of the 2^+ state in ^{48}Ca is due to a rather good $1f_{7/2}$ shell closure, and the relatively high energy for the 2^+ state in ^{52}Ca is due to a partial shell closure for the $2p_{3/2}$ shell. Beyond ^{52}Ca the effective single-particle energies of the $2p_{1/2}$ and $1f_{5/2}$ orbits are close and there are no other shell effects until the ^{60}Ca closed shell. In nuclides around ^{60}Ca the $1g_{9/2}$ orbit may become important but this is not included in the model space and there is no experimental information available.

For higher Z the shell-model calculation in the full *pf* shell quickly becomes intractable because of the large dimensions. In a few cases such as ^{56}Ni the Monte-Carlo shell-model has been used [16] (for which the FPD6

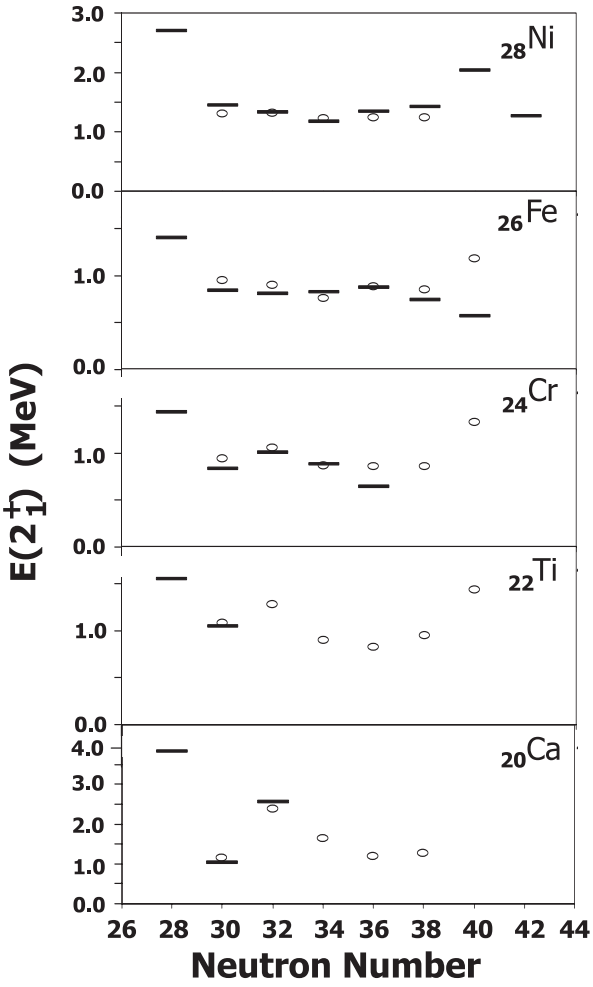

Figure 2: $E(2_1^+)$ sytematics for neutron-rich nuclides between $20 \leq Z \leq 28$. The experimental $E(2_1^+)$ values are denoted by dashes, where the data was obtained from Ref. [8, 9, 10, 11]. The open circles represent $E(2_1^+)$ values obtained from truncated shell-model calculations. See text for details.

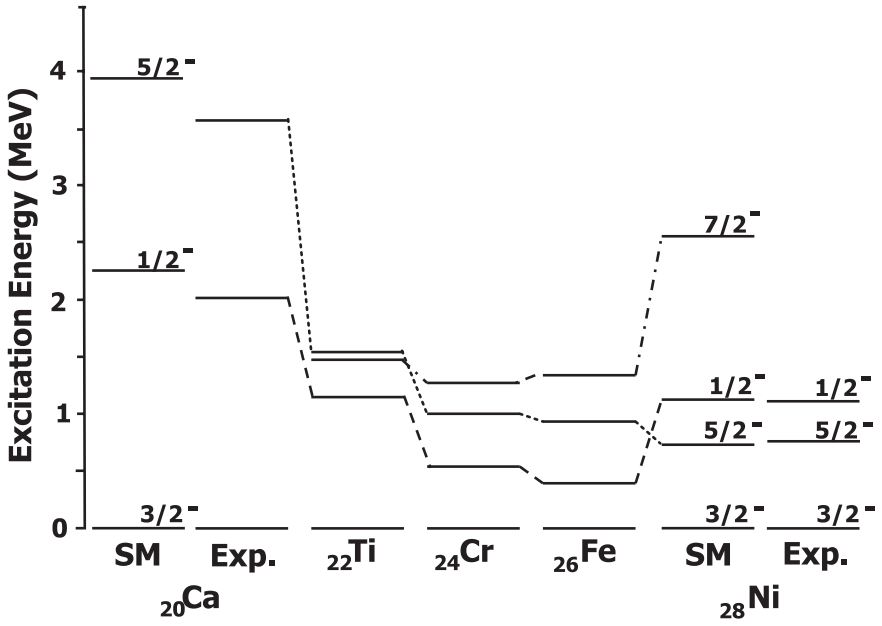

Figure 3: Low-energy states for the odd-A $N = 29$ isotones in the range $20 \leq Z \leq 28$ [9]. Shell-model results for ^{49}Ca and ^{57}Ni are also depicted.

interaction still gives a good spectrum). However, the good closure of the $1f_{7/2}$ shell at ^{48}Ca means that to a good approximation the nuclei beyond $N = 28$ may be treated as neutrons in the ($2p_{3/2}$, $2p_{1/2}$, $1f_{5/2}$) model space. When this truncation is made for the Ca isotopes the energies of the 2^+ states (see Fig. 2) and their wave functions are close to those of the full space, which includes $1f_{7/2}$. (These truncated calculations use as inputs the single-particle levels in ^{49}Ca as obtained from FPD6 which are close to the experimental values.) For higher Z there is clear evidence of the dominance of the $1f_{7/2}$ shell for protons in the 0^+, 2^+, 4^+, 6^+ spectra of ^{50}Ti, ^{52}Cr and ^{54}Fe. ^{56}Ni shows a partial $1f_{7/2}$ shell closure (e.g. the relatively high 2^+ energy). Thus for protons the model space is truncated to the pure $1f_{7/2}$ shell with the proton two-body interaction taken as a function of Z to match exactly the 0^+, 2^+, 4^+, 6^+ spectra of ^{50}Ti, ^{52}Cr and ^{54}Fe. The neutron single-particle energies are linearly interpolated between ^{49}Ca and ^{57}Ni such that the spectrum of single-particle states in ^{57}Ni is reproduced. This defines the input to the shell-model interpretation of the 2^+ energies.

Figure 3 depicts the low-energy level structure for the odd A, $N = 29$ isotones within the vicinity $20 \leq Z \leq 28$, where data was taken from Ref. [9]. For comparison, the levels predicted via shell-model calculations for ^{49}Ca and ^{57}Ni are also shown. The energies of the $3/2^-$, $1/2^-$ and $5/2^-$ states follow the general behavior of the $\nu 2p_{3/2}$, $\nu 2p_{1/2}$ and $\nu 1f_{5/2}$ orbitals, respectively. At $Z = 20$, a substantial gap is observed between the $\nu(2p_{1/2} - 1f_{5/2})$ and the $\nu(2p_{3/2} - 2p_{1/2})$ orbitals. The existence of these gaps suggest an $N = 32$ and possibly an $N = 34$ subshell for calcium isotopes. As protons begin to fill the $1f_{7/2}$ orbital, the $5/2^-$ state is lowered. By Ni, the $\pi 1f_{7/2}$ - $\nu 1f_{5/2}$ interaction is maximum and draws the $\nu 1f_{5/2}$ orbital below $\nu 2p_{1/2}$, which eliminates $N = 32$ subshell closure.

a. Department of Physics, Florida State University, Tallahassee, Florida 32306.
b. Department of Physics, University of Notre Dame, Notre Dame, Indiana 46556

References

1. F. Tondeur, *Nuclei Far From Stability 4*, Helsingor, CERN Report 81-09 (1981) 81.
2. A. Huck *et al.*, Phys. Rev. C **31** (1985) 2226.
3. R. Chapman, S. Hinds and A.E. Macgregor, Nucl. Phys. **A119** (1968) 305.
4. T.T. Bardin *et al.*, Phys. Rev. C **14** (1976) 1782.
5. J.I. Prisciandaro *et al.*, *Annual Report 2000:National Superconducting Cyclotron Laboratory.*
6. O. Sorlin *et al.*, Nucl. Phys. **A632** (1998) 205.
7. F. Ameil *et al.*, Eur. Phys. J. **A1** (1998) 275.
8. J.I. Prisciandaro *et al.*, Phys. Lett. B **510** (2001) 17.
9. R.B. Firestone, **Table of Isotopes**, Eighth Edition, Volume 1, (John Wiley & Sons, New York, 1996).
10. O. Sorlin *et al.*, Nucl. Phys. **A669** (2000) 351.
11. M. Hannawald *et al.*, Phys. Rev. Lett. **82** (1999) 1391.
12. X.L. Tu *et al.*, Z. Phys. **A337** (1990) 361.
13. P. Federman and S. Pittel, Phys. Lett. **69B** (1977) 385.
14. G. Cata *et al.*, Z. Phys. **A335** (1990) 271.
15. W.A. Richter *et al.*, Nucl. Phys. **A523** (1991) 325.
16. T. Mizusaki *et al.*, Phys. Rev. C **59** (1999) R1846.